Available online www.ejaet.com

European Journal of Advances in Engineering and Technology, 2023, 10(5): 9-14

Research Article ISSN: 2394 - 658X

Simulation and Optimization of CZTS-based Photovoltaic Devices: Effect of Deposition Temperature on Cell performance

B. NDIAYE[1], E. M. KEITA[1], M. NDIAYE[2], M. S. MANE[1], A. SAGNA[2], B. MBOW[1] and C. SENE[1]

[1]Laboratoire des Semiconducteurs et d'Energie Solaire, Département de Physique, Faculté des Sciences et Techniques, Université Cheikh Anta Diop, Dakar, Sénégal
[2]Hydraulics, Rural Engineering, Machinery and Renewable Energies Training and Research Unit, University of Sine Saloum El Hadj Ibrahima NIASS, Kaolack, Senegal
Corresponding author: manesolmats@yahool.fr

ABSTRACT
Kesterite Cu_2ZnSnS_4 (CZTS) thin absorber layers are used in PV devices particularly in the CIGS solar cell like-structure where the CIGS component is replaced by the earth-abundant and non-toxic CZTS absorber layer. In this theoretical study we investigate the effect of the growth temperature on the quantum efficiency of the CZTS-based solar cell. For this purpose, Cu_2ZnSnS_4 thin films grown using the simple and low-cost Close Spaced Vapor Transport (CSVT) process are considered. Numerical models based on solving continuity equation with conditions at the appropriate limits are used to determine the contributions of each part of the device to the total photocurrent. The evolution of the internal quantum yield of the device was then monitored according to substrate temperature during the kesterite layer deposition. The results can provide important guideline for high-efficiency thin CZTS solar cells manufactured by the CSVT deposition process.

Key words: kesterite, solar cells, thin films, quantum efficiency, photovoltaics

---

INTRODUCTION

The thin layer technology is developed in photovoltaic conversion to produce low-cost and efficient modules. The inherent benefits of this technology, particularly the low material consumption, the direct preparation of semiconductors by simple processes on low-cost supporting materials without using other costly formatting steps such as machining, make it a particularly attractive route for the development of photovoltaic cells. Intensive researches have been carried out on properties exploration of a large number of materials, with the major objective of obtaining low-cost highly efficient photovoltaic cells with high stability.

From all of these materials, polycrystalline thin CdTe films and copper-based chalcopyrite thin-films, the reference of which is copper and indium diselenide $CuInSe_2$ (CIS), emerged. These materials have exceptional characteristics making them particularly suitable for low-cost photovoltaic applications. Furthermore, the CIS-based PV devices are greatly improved by cationic and/or anionic substitution leading to $Cu(In,Ga)Se_2$ (CIGS), $Cu(In,Ga)(Se,S)_2$, etc. Efficiencies up to 22.6 % were achieved with copper, indium, gallium diselenide (CIGS) cells [1]. In spite of these high efficiencies and the existence of routes for their further improvement, competitiveness of thin CIGS-based technology with others technologies can be affected by the scarcity and high price of indium.

To fully benefit from advantages of the low manufacturing cost in the thin-film solar cell technology, researches on CZTS kesterite materials that are made up of non-toxic, cheap and earth abundant chemical elements have received particular attention in recent years. [2].

The p-type CZTS thin films have an ideal direct band gap approximately 1 eV [3, 4]. Their absorption coefficients are as high as those of CIGS thin absorber layers. They reach values higher than 10^4 cm^{-1} for photon energy above 1 eV [5].

Furthermore, based on Shockley-Queisser limit, the maximum theoretical efficiency of the CZTS-based solar cell is about 32.2% [6, 7]. This make them very attracting alternative candidates to polycrystalline CdTe and CIGS based solar cells. However, power conversion efficiencies of CZTS-based solar cells are low, ~13% at laboratory scale,

indicating that many improvements are necessary to be performed to reduce the difference between theoretical and current values of efficiencies. Key issues that need to be addressed to reduce this discrepancy in efficiency include absorber, buffer and windows layer qualities as well the quality of the various interfaces in the solar cell. Recombination processes occur in the space charge layer of the junction, in the bulk material of the various components of the solar cell and at the different interfaces. These recombination phenomena have very harmful consequences on both the short circuit current and the open circuit voltage of the devices due to their effects on current collection and forward bias injection current voltage.

Absorber layer properties include optical properties, presence of secondary phases, defect concentration, grain boundaries, electronic and band structure, etc., which depend particularly on the deposition method. The CSVT deposition method which is a variant of the thermal evaporation deposition technique, has been shown to produce high quality CZTS absorber layers free of secondary phases. Substrate temperature during film growth on the CZTS thin properties have been investigated [8]. In this study a numerical model is presented to provide insights in the quantum efficiency of the CSVT-CZTS based solar cells with the intent of clarifying the effect of substrate temperature during film growth. The main objective of this study is to obtain a high efficiency CSVT-CZTS based solar cell. The computational results based on solving the steady-state continuity equation and Poisson's equation accounted for the contributions of the different parts of the solar cell to the photocurrent as well as the internal quantum performance. The evolution of the internal quantum efficiency was then monitored according to substrate temperature during the active layer growth.

EXPERIMENTAL DETAILS AND CALCULATION MODELS

Experimental Details

The Cu_2ZnSnS_4 (CZTS) thin films were grown on soda-lime glass substrates by the simple and low-cost Close Spaced Vapor Transport (CSVT) method. Experimental details have been described elsewhere [8]. Films characterizations exhibited the kesterite structure of CZTS layers with a (112) plane preferred orientation [8]. Furthermore, they highlighted a p-type conductivity and proved that control over film growth temperature is a critical factor for obtaining good structural, optical, chemical and electrical CZTS layers. The CZTS films used in this study were deposited with substrate temperature controlled in range from 460 °C – 540 °C [9].

Absorption coefficients were calculated from transmission spectra of three CZTS samples deposited at 460°C, 500°C and 540°C. The optical band gaps of these CZTS films were estimated to be 1.34 eV, 1.48 eV and 1.52 eV, respectively [9]. Other parameters such as carrier concentrations, mobility and resistivity are given in following table.

Table 1: Electrical properties of the CZTS thin films obtained at different substrate temperatures. [9]

Substrate temperatures (°C)	**Carrier concentration (cm^{-3})**	**Mobility ($cm^2/V.s$)**	**Resistivity (Ω.cm)**
460	$1.2x10^{18}$	1.4	3.76
500	$3.4x10^{17}$	6.4	2.87
540	$2x10^{17}$	2.5	8.19

The thin film solar cell structure in figure 1 is considered. In this structure the polycrystalline CZTS active film is deposited on a thin Mo followed by CdS buffer and ZnO window layers depositions.

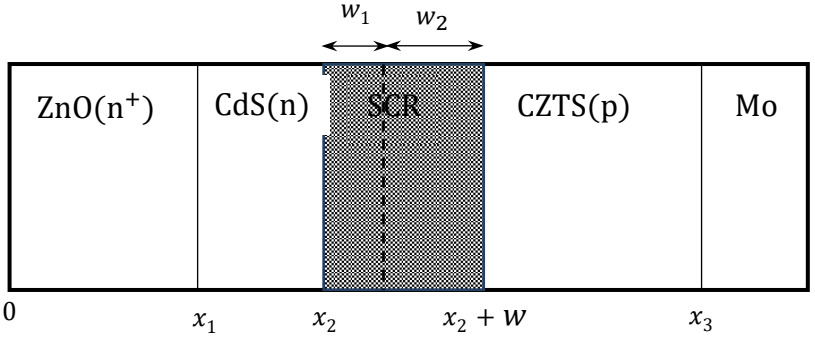

Figure 1: Diagram of the structure ZnO/CdS/CZTS/Mo solar cell.

The performance of a solar cell can be quantified by internal and external quantum efficiencies. For this purpose a calculation model is used in this study. In this theoretical model, absorption coefficients of the different components of the structure, geometrical and electrical parameters of the device including diffusion lengths of charge carriers, recombination velocities at both front and rear surfaces as well as at the interface between the different layers, thicknesses of these layers, etc., are introduced.

For CZTS thin layers, absorption coefficient are obtained from transmission spectra recorded for films grown at 460° C, 500 °C and 540 °C. Optical reflection coefficients at each interface in the spectral range used are neglected. It is also considered that the space charge region is located only between the p and n regions of the structure and there is no electric field outside this region. Moreover, in this same region, recombination phenomena are neglected.

Calculation Model

Photocurrent Calculation in the Window Layer

In the window layer (ZnO), where the minority carriers are the holes, the continuity equation is given by:

$$\frac{d^2\Delta p_1}{dx^2} - \frac{\Delta p_1}{L_{p_1}^2} = \frac{-\alpha_1 F(1-R)e^{-\alpha_1 x}}{D_{p_1}} \quad (1)$$

where Δp_1 is the hole density, D_{p_1} and L_{p_1} are the hole diffusion coefficient and hole diffusion length respectively. And the boundary conditions defined as follows:

$$D_{p_1}\left(\frac{d\Delta p_1}{dx}\right) = S_{p_1}\Delta p_1 \;\; for\; x = 0 \quad (2)$$

$$\Delta n_1 = 0 \;\; for\; x = x_1 \quad (3)$$

The photocurrent's expression at x_1 depth is then given by:

$$J_{p_1}(x_1) = \frac{-q\,\alpha_1 F(1-R)L_{p_1}}{(\alpha_1^2 {L_{p_1}}^2 - 1)}\left[\frac{\left(\frac{S_{p_1}L_{p_1}}{D_{p_1}} + \alpha_1 L_{p_1}\right) - e^{-\alpha_1 x_1}\left[\frac{S_{p_1}L_{p_1}}{D_{p_1}} ch\left(\frac{x_1}{L_{p_1}}\right) + sh\left(\frac{x_1}{L_{p_1}}\right)\right]}{\frac{S_{p_1}L_{p_1}}{D_{p_1}} sh\left(\frac{x_1}{L_{p_1}}\right) + ch\left(\frac{x_1}{L_{p_1}}\right)} - \alpha_1 L_{p_1} e^{-\alpha_1 x_1}\right] \quad (4)$$

$x_1$and α_1 are the thickness and the absorption coefficient of the ZnO layer, respectively. S_{p_1} is the surface recombination velocity, respectively. This photocurrent is essentially due holes.

Photocurrent Calculation in the Buffer Layer

In the bulk buffer layer (CdS), the photocurrent is also a hole current, which results from the contribution of regions 1 and 2 taking into the interface effect characterized by a recombination rate at the interface noted S_{p_2}. The continuity equation is given by:

$$\frac{d^2\Delta p_2}{dx^2} - \frac{\Delta p_2}{{L_{p_2}}^2} = \frac{-\alpha_2 F(1-R)e^{-\alpha_1 x_1}e^{-\alpha_2(x-x_1)}}{D_{p_2}} \quad (5)$$

and boundary conditions expressed as:

$$D_{p_2}\frac{d\Delta p_2}{dx} = S_{p_2}\Delta p + D_{p_1}\frac{d\Delta p_1}{dx} \;\; for\; x = x_1 \quad (6)$$

$$\Delta n_2 = 0 \;\; for\; x = x_2 \quad (7)$$

The photocurrent obtained by $J_{p_2} = qD_{p_2}\left.\frac{d\Delta p_2}{dx}\right|_{x=x_2}$ has the following expression:

$$J_{p_2}(x_2) = \left[\frac{q\alpha_2 F(1-R)L_{p_2}e^{-\alpha_1 x_1}}{\left(\alpha_2{}^2 {L_{p_2}}^2 - 1\right)}\right]$$
$$\left[\frac{\left(\frac{S_{p_2}L_{p_2}}{D_{p_2}} + \alpha_2 L_{p_2}\right) - e^{-\alpha_2(x_2-x_1)}\left[\frac{S_{p_2}L_{p_2}}{D_{p_2}} ch\left(\frac{x_2-x_1}{L_{p_2}}\right) + sh\left(\frac{x_2-x_1}{L_{p_2}}\right)\right]}{\frac{S_{p_2}L_{p_2}}{D_{p_2}} sh\left(\frac{x_2-x_1}{L_{p_2}}\right) + ch\left(\frac{x_2-x_1}{L_{p_2}}\right)} - \alpha_2 L_{p_2} e^{-\alpha_2(x_2-x_1)}\right] +$$
$$\frac{J_{p_1}(x_1)}{\frac{S_{p_2}L_{p_2}}{D_{p_2}} sh\left(\frac{x_2-x_1}{L_{p_2}}\right) + ch\left(\frac{x_2-x_1}{L_{p_2}}\right)} \quad (8)$$

where Δp_2 is the hole density, D_{p_2} and L_{p_2} are the hole diffusion coefficient and hole diffusion length respectively, S_{p_2} is the surface recombination velocity.

Photocurrent in the Space Charge Region

In the region $x_2 \le x \le x_2 + w_1$, charges recombination is neglected. It is assumed that the transit time of free carriers in this zone is much less than their lowest lifetimes because of the strong electric field there [50]. They will not have time to recombine and then are all collected. The expression of the electron photocurrent is given by:

$$J_{ZCE} = qF(1-R)e^{-\alpha_1 x_1}e^{-\alpha_2(x_2-x_1)}[e^{-\alpha_2 w_1} - 1] + qF(1-R)e^{-\alpha_1 x_1}e^{-\alpha_2[(x_2+w_1)-x_1]}[e^{-\alpha_3 w_2} - 1] \quad (9)$$

Photocurrent Calculation in the CZTS-Base Layer $x_2 + w \le x \le x_3$

In the region 3 (absorber layer (CZTS)), where the minority carriers are electrons, the continuity equation is written:

$$\frac{d^2\Delta n_3}{dx^2} - \frac{\Delta n_3}{L_{n_3}^2} = -\frac{\alpha_3}{D_{n_3}}F(1-R)e^{-\alpha_1 x_1}e^{-\alpha_2[(x_2+w_1)-x_1]}e^{\alpha_3(x_2+w_1)}e^{-\alpha_3 x} \quad (10)$$

The boundary conditions are written as follows:

$$D_{n_3}\frac{d\Delta n_3}{dx} = -S_{n_3}\Delta n_3 \;\; fo\; x = H \quad (11)$$

$$\Delta p_3 = 0 \;\; for\; x = x_2 + w \quad (12)$$

The electron photocurrent given by $J_{n_3} = -q\,D_{n_3}\left.\frac{d\Delta n_3}{dx}\right|_{x=x_2+w}$, is expressed by:

$$J_{n_3}(x_2+w)=\frac{q\alpha_3 L_{n_3}\,F(1-R)e^{[(\alpha_2-\alpha_1)x_1]}\,e^{[(\alpha_3-\alpha_2)(x_2+w_1)]}}{\left(\alpha_3^2L_{n_3}^2-1\right)}\times$$
$$\left\{\frac{\left(\alpha_3L_{n_3}-\frac{S_{n_3}L_{n_3}}{D_{n_3}}\right)e^{-\alpha_3x_3}+e^{-\alpha_3(x_2+w)}\left\{\frac{S_{n_3}L_{n_3}}{D_{n_3}}ch\left[\frac{x_3-(x_2+w)}{L_{n_3}}\right]+sh\left[\frac{x_3-(x_2+w)}{L_{n_3}}\right]\right\}}{\frac{S_{n_3}L_{n_3}}{D_{n_3}}sh\left[\frac{x_3-(x_2+w)}{L_{n_3}}\right]+ch\left[\frac{x_3-(x_2+w)}{L_{n_3}}\right]}-\right.$$
$$\left.\alpha_3L_{n_3}e^{-\alpha_3(x_2+w)}\right\} \quad (13)$$

where Δn_3 is the electron density, D_{n_3} and L_{n_3} are the electron diffusion coefficient and electron diffusion length respectively, S_{n_3} is the surface recombination velocity.

Total Photocurrent Calculation

The total photocurrent results from the contribution of the different regions of the structure. It can therefore be expressed as follows:

$$J_{ph}=\left|J_{p_2}(x_2+w)\right|+\left|J_g(x_2+w)\right|+\left|J_{n_3}(x_2+w)\right| \quad (14)$$

Internal Quantum Efficiency

For this analytical study, we developed the collection efficiency model for thin-film solar cells and established its mathematical expression. The developed model is applied to determine the internal quantum efficiency which is the ratio of the number of charge carriers collected by the photovoltaic device to the number of photons of a given wavelength or energy on the device [32]. Internal quantum efficiencies named $\eta_2, \eta_3, \eta_g \; and \; \eta_{tot}$ are defined as follows:

$$\eta_2=\frac{\left|J_{p_2}(x_2+w)\right|}{|qF(1-R)|} \quad (15)$$

$$\eta_3=\frac{\left|J_{n_3}(x_2+w)\right|}{|qF(1-R)|} \quad (16)$$

$$\eta_g=\frac{\left|J_g(x_2+w)\right|}{|qF(1-R)|} \quad (17)$$

$$\eta_{tot}=\frac{|J_{ph}|}{|qF(1-R)|}=\frac{\left|J_{p_2}(x_2)\right|+\left|J_g(x_2+w)\right|+\left|J_{n_3}(x_2+w)\right|}{|qF(1-R)|} \quad (18)$$

RESULTS AND DISCUSSIONS

In our study, we are interested here in the influence of the temperature of the substrate during the deposition on the characteristics of the layers of CZTS and the performances of the modules obtained.

Effect of Substrate Temperature on the Internal Quantum Efficiency of the Cell

The curves of variation of the quantum efficiency according to the energy of the photon for various temperatures of the substrate is plotted.

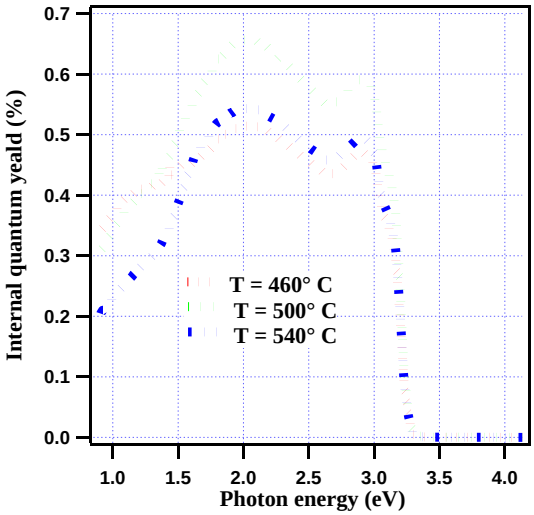

Fig. 2 Internal quantum efficiency as a function of deposition temperature

An increase in efficiency is observed when the temperature of the substrate increases for energies slightly greater than 1.5 eV.

If the substrate temperature becomes too high, the performance of the cell drops.

At low temperatures, the efficiency is affected by the existence of secondary phases such as Cu_2SnS_3 and defects such as Cu_{Zn}, Zn_{Cu}, Cu_{Zn} and Sn_{Zn}.

If the temperature is too high, the layers obtained have a very large gap which limits the performance of the devices obtained. This rise in the gap is linked to:

- The formation of binary phases made up of zinc and sulfur which form under these conditions. The layers are poor in copper and rich in zinc at high temperatures. The formation of the ZnS phase is then observed. This binary has a high gap of the order of 3.5 eV. It then behaves like an insulator which leads to a drop in cell performance. We can also observe the formation of tin sulphide SnS_2 which has a gap of about 2.2 eV. It can behave as an insulator or a semiconductor of opposite polarity to that of CZTS.
- The existence of Zn_{Cu}+VCu defect complexes which promote an increase in the gap. According to D. A. R. Barkhouse et al [10] these defects lead to an increase in the gap.

An increase in the gap with the temperature of the substrate is also noted in other works. In [11]
Y. Arba et al obtained a gap which reached 2.12 eV for a substrate temperature of 425°C. This increase in the gap would be due to the formation of secondary compounds such as the copper sulphide Cu_2S whose gap is close to 2 eV.
The impact of substrate temperature on the properties of CZTS thin films is also studied in other publications. The ultrasonic spray method is used by W. Daranfed et al. It is an easy and inexpensive method that gives very smooth, uniform and homogeneous layers [12].
He notes an increase in the value of the gap with the temperature of the substrate from 320°C. This may be due to the better crystallization obtained at high temperatures. It also indicates that at high deposition temperatures, the layers are poor in copper and rich in zinc. The formation of high-gap binaries such as ZnS inevitably leads to an increase in the gap of the material.
The previous curves also allow us to see the evolution of the yield as a function of the thickness of the CZTS layer.

Effect of Substrate Temperature on Base Contribution

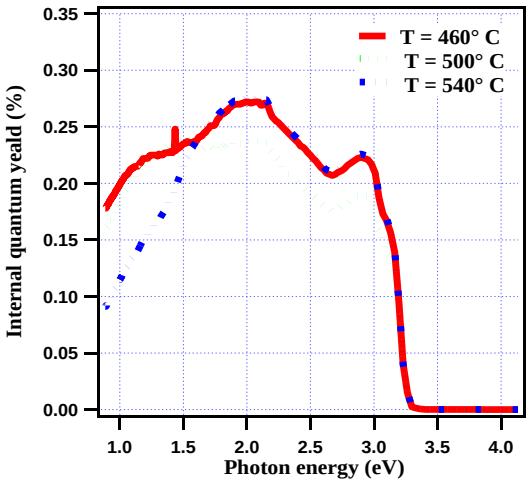

Fig. 3 Contribution of the base as a function of the deposition temperature

The contribution of the base to the quantum efficiency is weak. It can be seen that it increases with the temperature of the substrate to reach a ceiling of the order of 0.275% from 500°C.
The low contribution of the base would be due to a high recombination rate in this area.

Effect of Substrate Temperature on Space Charge Area Contribution.

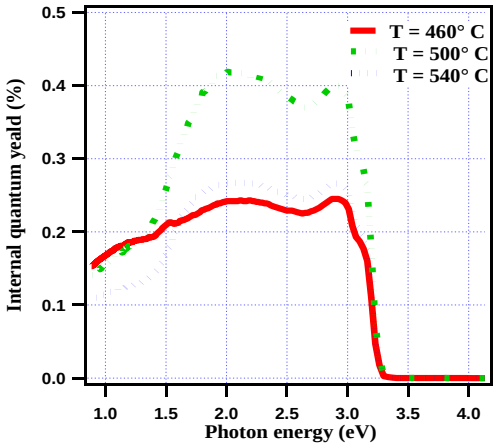

Fig. 4 Contribution of the space charge area as a function of the deposition temperature

The contribution of the charge and space area is more important than that of the base.
For a photon energy of the order of 2 eV, the contribution is greater for a substrate temperature of 500 °C.
Maykel Courel et al studied the contributions of the different parts of the cell on the efficiency. They also find that the contribution of the charge space region is more important because the absorption is greater in this region [14].

CONCLUSION

This work allowed us to calculate the contributions of the different parts of the cell to the total photocurrent. The expression of the total photocurrent led to the total performance of the cell. The influence of substrate temperature on devices is studied. At low temperatures the layers are rich in copper and poor in zinc. Secondary phases such as CTS and defects justify the value of the gap below the usual CZTS gap of 1.5 eV. We then have low efficiencies. The increase in temperature gives zinc-rich layers and copper-poor layers. Secondary high gap compounds and defects are formed which cause the material gap to increase. At the same time, there is an improvement in the gap up to 500°C. From this value the excess value of the gap leads to a decrease in efficiency.
The results of this study show that the best devices are obtained with a substrate temperature of 500 °C.

REFERENCES

[1]. P. Jackson, R. Wuerz, D. Hariskos, E. Lotter, W. Witte, M. Powalla, “Effects of heavy alkali elements in Cu(In,Ga)Se_2 solar cells with efficiencies up to 22.6%”, Phys. Status Solidi - Rapid Res. Lett. 10 (2016) 583–586.
[2]. K. Tanaka, N. Moritake, M. Oonuki, H. Uchiki, Japanese Journal of Applied Physics, 47, 598 (2008).
[3]. M. Grossberg, J. Krustok, K. Timmo, M. Altosaar, Radiative recombination in $Cu_2ZnSnSe_4$ monograins studied by photoluminescence spectroscopy, Thin Solid Films 517 (2009) 2489.
[4]. S. Siebentritt, S. Schorr, Kesterites—a challenging material for solar cells, Prog. Photovoltaics: Res. Appl. 20 (2012) 512.
[5]. Kentaro Ito, Tatsuo Nakazawa, Electrical and optical properties of stannite type quaternary semiconductor thin films, Jpn. J. Appl. Phys. 27 (1988) 2094
[6]. Katagiri, H.; Jimbo, K.; Maw, W.S.; Oishi, K., “Development of CZTS-based thin film solar cells”, Thin Solid Films 2009, 517, 2455–2460.
[7]. Kahraman, S.; Çetinkaya, S.; Podlogar, M.; Bernik, S. “Effects of the sulfurization temperature on sol gel-processed Cu_2ZnSnS_4 thin films”, Ceram. Int. 2013, 39, 9285–9292.
[8]. Alphousseyni SAGNA ‘‘Etude et élaboration par Close-Spaced Vapor Transport (CSVT), d'absorbeurs Cu_2ZnSnS_4 en couches minces polycristallines destinés à la réalisation de photopiles à faible coût’’ thèse soutenue le 03/12/2016.
[9]. Sagna, K. Djessas, C. Sene, M. Belaqzizd, H. Chehouanid, O. Briote, M. Morete “Growth, structure and optoelectronic characterizations of high quality Cu_2ZnSnS_4 thin films obtained by close spaced vapor transport” Super-réseaux et Microstructures (2015).
[10]. D. A. R. Barkhouse, O. Gunawan, T. Gokmen, T. K. Todorov, and D. B. Mitzi, “Device characteristics of a 10.1% hydrazine-processed $Cu_2ZnSn(Se,S)_4$ solar cell: Characteristics of a 10.1% efficient kesterite solar cell,” Prog. Photovolt. Res. Appl., vol. 20, no. 1, pp. 6–11, Jan. 2012.
[11]. Y. Arba*, M. Rafi, H. Tchognia, B. Hartiti, A. Ridah, P. Thevenina, ‘‘Effect of substrate temperature on physical properties of CZTS thin films’’, Journal of optoelectronics and advanced materials Vol. 15, No. 11 - 12, p. 1200 – 1203, November – December 2013.
[12]. W. Daranfed, R. Fassi, A. Hafdallah, F. Ynineb, N. Attaf, M.S. Aida, L. Hadjeris, H. Rinnert and J. Bougdira, ‘‘Substrate effect temperature on Cu_2ZnSnS_4 thin films deposited by ultrasonic technique’’, Journal of New Technology and Materials JNTM Vol. 01, N°00 (2011) 44-46.
[13]. Oubouchou Amina: ‘‘Etude et simulation d’une cellule solaire à base de couches minces CZTS’’ Mémoire de Master (2018-2019) Université Saad Dahlab de BLIDA, Algérie.
[14]. Maykel Courel, F.A. Pulgarin-Agudelo, J.A. Andrade-Arvizu, O. Vigil- Galan, “Open-circuit voltage enhancement in CdS/$Cu_2ZnSnSe_4$ based thin film solar cells: A metal-insulator-semiconductor (MIS) performance”, solar energy materials and solar cells 149 (2016) 204-212.